View metadata, citation and similar papers at core.ac.uk
brought to you by CORE
provided by CiteSeerX

Proceedings of GT2006
ASME Turbo Expo 2006: Power for Land, Sea and Air
May 8-11, 2006, Barcelona, Spain

GT2006-91234

ON NEAR-WALL DYNAMIC COUPLING OF LES WITH RANS TURBULENCE MODELS

Goéric Daeninck
Mechanical Engineering Department
Université catholique de Louvain
B-1340 Louvain-la-Neuve
Belgium
Email: daeninck@term.ucl.ac.be

Gorazd Medic*
Mechanical Engineering Department
Stanford University
Stanford, CA 94305
Email: gmedic@stanford.edu

Jeremy A. Templeton
Mechanical Engineering Department
Stanford University
Stanford, CA 94305
Email: temple@stanford.edu

Georgi Kalitzin
Mechanical Engineering Department
Stanford University
Stanford, CA 94305
Email: kalitzin@stanford.edu

ABSTRACT

In this paper, the RANS/LES coupling formulation proposed in [1–3] is adapted for various RANS turbulence models. In that formulation, the LES subgrid-scale eddy-viscosity is replaced in the near-wall region with a RANS eddy-viscosity dynamically corrected with the resolved turbulent stress. The RANS eddy-viscosity is first obtained from precomputed tables. To further generalize the approach, RANS turbulence model equations (for Spalart-Allmaras and k-ω) are then solved simultaneously with the LES. Detailed results are presented for channel flow at $Re_\tau = 395$ and compared to traditional LES. The method is then applied to a serpentine passage and compared with DNS computations [4] at $Re_\tau = 180$.

INTRODUCTION

In recent years, there is a growing trend to apply computational techniques to turbomachinery flows of increased complexity, including unsteady and three-dimensional effects. Significant efforts have been put into combining Reynolds-averaged Navier Stokes (RANS) techniques with the more accurate large-eddy simulation (LES) framework. On wall-resolved grids, LES is able to capture the small near-wall turbulent scales, albeit at a high computational cost [5].

Several methods have been proposed to reduce the computational cost. One such approach is to avoid resolving the near-wall layer altogether by applying wall models which provide wall stress boundary conditions to LES. Such methods have been used by [6–8] with some success, although they underpredict the mass flow rate in channel flow. Another approach involves the use of grids coarsened in the wall-parallel direction, while leaving the wall-normal resolution unchanged. Not all turbulent scales can be resolved with such grids and additional modeling is required. RANS equations are well suited for these type of grids because only the mean wall-normal gradients must be resolved while the entire turbulence spectrum is modeled. A well-known approach in this category is detached-eddy simulation (DES) which was designed to simulate massively separated aerodynamic flows. In this technique, RANS is used in the boundary layer while LES resolves the separated region [9]. However, in pressure-driven channel flow DES overpredicts the

*Address all correspondence to this author.

Copyright © 2006 by ASME

Downloaded From: https://proceedings.asmedigitalcollection.asme.org on 07/01/2019 Terms of Use: http://www.asme.org/about-asme/terms-of-use

mass flow rate, as discussed in [10].

A novel concept for the near-wall treatment of LES has been presented in [1–3]. It has been applied successfully to channel flow with both a wall model and wall-parallel coarsening. In that formulation, the LES subgrid-scale eddy-viscosity is replaced in the near-wall region with a RANS eddy-viscosity dynamically corrected with the resolved turbulent stress. The RANS eddy-viscosity was precomputed from the RANS equation for channel flow using the averaged velocity profile from the LES and stored in a look-up table.

In this paper, the proposed RANS/LES coupling formulation is adapted for various RANS turbulence models. First, the results computed with the LES-based table for RANS eddy-viscosity are compared to computations with tables precomputed using k-ω [11] and Spalart-Allmaras [12] models. In order to further generalize the formulation, the RANS eddy-viscosity is computed from RANS equations solved simultaneously with the LES. The specific issues on how to couple these two simulations are addressed here. Detailed results are presented for channel flow at $Re_\tau = 395$ and compared to traditional LES. Finally, this approach is applied to a serpentine passage and compared with DNS computations [4] at $Re_\tau = 180$.

NEAR-WALL RANS/LES COUPLING

LES equations for the filtered velocity $\hat{u}_i$ are solved throughout the entire computational domain:

$$\frac{\partial \hat{u}_i}{\partial t} + \frac{\partial (\hat{u}_j \hat{u}_i)}{\partial x_j} = -\frac{1}{\rho}\frac{\partial \hat{p}}{\partial x_i} + \frac{\partial}{\partial x_j}\left((\nu + \nu_t^{SGS})(\frac{\partial \hat{u}_i}{\partial x_j} + \frac{\partial \hat{u}_j}{\partial x_i}) \right) \quad (1)$$

$$\frac{\partial \hat{u}_j}{\partial x_j} = 0 \quad (2)$$

In the near-wall region, typically over a dozen of computational cells, the instantaneous SGS eddy-viscosity is replaced by a RANS eddy-viscosity corrected using the resolved turbulent stress:

$$\nu_t^{SGS,NW} = \nu_t^{rans} + \overline{\hat{u}\hat{v}} / \frac{d\bar{\hat{u}}}{dy}. \quad (3)$$

where $\hat{u}$ and $\hat{v}$ are the streamwise and wall-normal velocity components. Since $\overline{\hat{u}\hat{v}}$ and $d\bar{\hat{u}}/dy$ have opposite signs, the second term on the right hand side of equation (3) is negative. Thus in the presence of turbulent fluctuations, the near-wall LES viscosity, $\nu_t^{SGS,NW}$, is always less than the RANS viscosity, ν_t^{rans}, with the difference being a dynamic correction for the resolved fluctuations. The RANS eddy-viscosity can be obtained from either

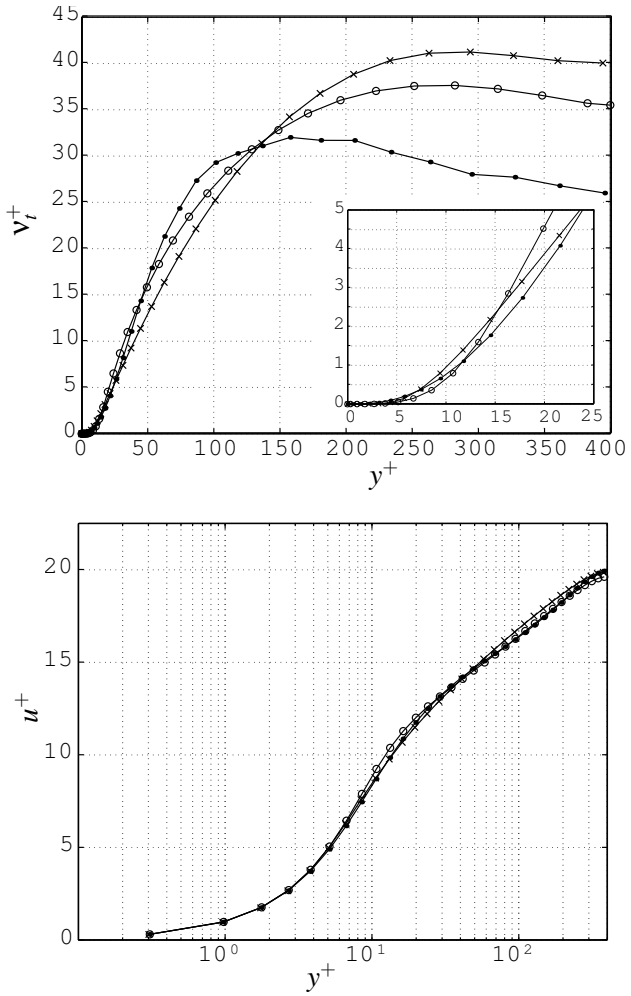

Figure 1. Channel flow at $Re_\tau = 395$. Precomputed tables for ν_t^{rans} (top) and the corresponding velocity profiles (bottom). Computations using ν_t^{rans} from LES (•), Spalart-Allmaras (○) and k-ω turbulence model (×).

precomputed look-up tables or from a simultaneous solution of RANS turbulence models. The velocity gradient, $d\hat{u}/dy$, and the turbulent stress, $\hat{u}\hat{v}$, come from the LES. The averaging operator can either be plane- or time-averaging. When using this approach, it is necessary to clip the eddy-viscosity (as is standard practice when using an SGS model, where the eddy-viscosity is clipped whenever its value drops below zero). Here, the eddy-viscosity is clipped at the level of the SGS model. The derivation of equation (3) for channel flow and additional discussion can be found in [1–3].

The LES code used in the computations is a second-order finite-volume method for solving the time-dependent three-dimensional incompressible Navier-Stokes equations in a generalized coordinate system [13]. The approach is based on the

Copyright © 2006 by ASME

Downloaded From: https://proceedings.asmedigitalcollection.asme.org on 07/01/2019 Terms of Use: http://www.asme.org/about-asme/terms-of-use

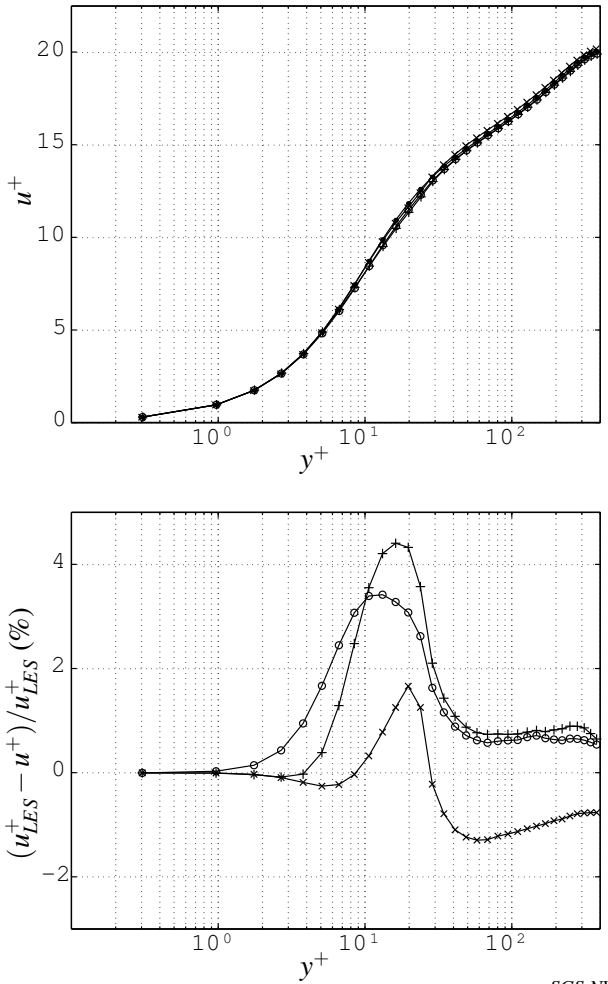

Figure 2. Channel flow at $Re_\tau = 395$. LES (•); LES + $\nu_t^{SGS,NW}$ with LES-based table for ν_t^{rans} (○); LES + $\nu_t^{SGS,NW}$ with Spalart-Allmaras table for ν_t^{rans} (×); LES + $\nu_t^{SGS,NW}$ with k-ω table for ν_t^{rans} (+). Top: u^+; Bottom: $(u^+_{LES} - u^+)/u^+_{LES}$ (in %).

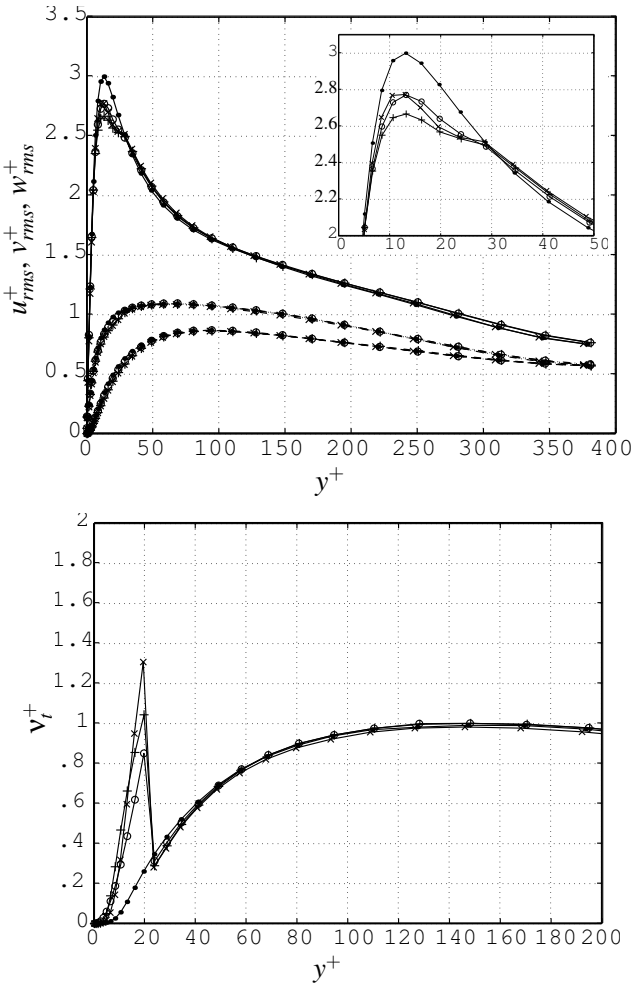

Figure 3. Channel flow at $Re_\tau = 395$. LES (•); LES + $\nu_t^{SGS,NW}$ with LES-based table for ν_t^{rans} (○); LES + $\nu_t^{SGS,NW}$ with Spalart-Allmaras table for ν_t^{rans} (×); LES + $\nu_t^{SGS,NW}$ with k-ω table for ν_t^{rans} (+). Top: rms velocities; Bottom: ν_t^+.

scheme developed in [14] where volume flux variables are used with the traditional time-splitting fractional step method. The equations are discretized using a staggered mesh system: the pressure is defined at the center of each cell and a volume flux is defined across each face. The method is limited to geometries which are complex in two directions while the third, spanwise direction must be treated using Cartesian coordinates and periodic boundary conditions. This type of boundary condition is also used in the streamwise direction and a source term is added to enforce a mean pressure gradient which drives the flow. The pressure gradient can be adjusted dynamically to maintain a constant mass flux through the channel. Wall Adapting Local Eddy-viscosity model (WALE) [15] is adopted as the subgrid scale model (for details, see Appendix B).

CHANNEL FLOW

The RANS/LES coupling is investigated for plane channel flow at $Re_\tau = u_\tau h/\nu = 395$. The channel dimensions are $2\pi h \times 2h \times \pi h$. A wall-resolved grid used in the computations consist of $80 \times 64 \times 64$ cells in the streamwise, wall-normal and spanwise directions, respectively, with the first cell centers at $y_1^+ = 0.3$.

Precomputed Tables For ν_t^{rans}

The RANS eddy-viscosity, ν_t^{rans}, used in the equation (3) to compute the near-wall eddy-viscosity $\nu_t^{SGS,NW}$, can be stored in precomputed look-up tables. These look-up tables are structured using a method similar to [16] for RANS wall functions.

The tables are constructed using several approaches. The first one uses an averaged velocity profile obtained from the

Copyright © 2006 by ASME

Downloaded From: https://proceedings.asmedigitalcollection.asme.org on 07/01/2019 Terms of Use: http://www.asme.org/about-asme/terms-of-use

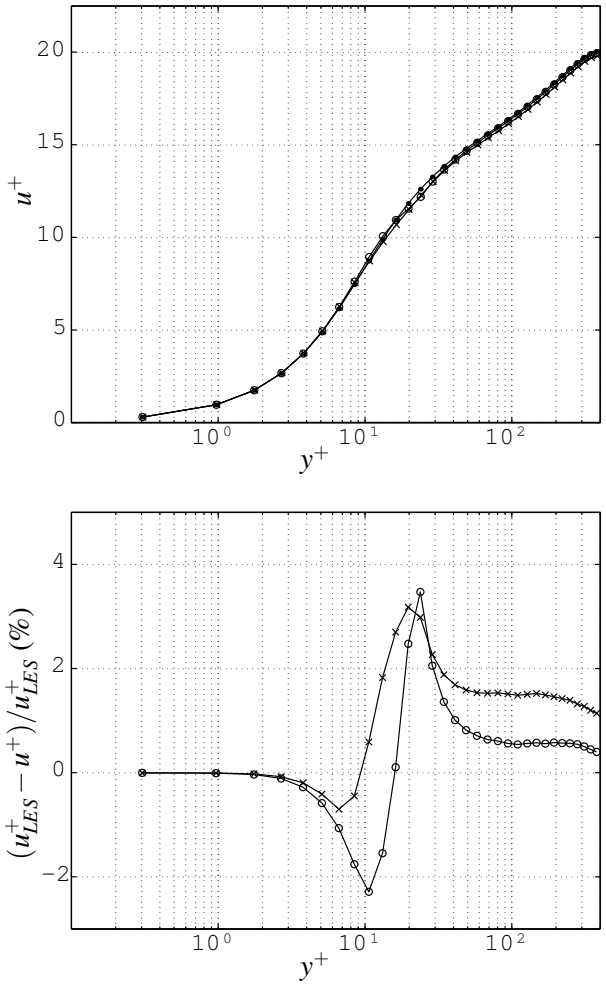

Figure 4. Channel flow at $Re_\tau = 395$. LES (•); LES dynamically coupled with Spalart-Allmaras model equations (○); LES dynamically coupled with k-ω model equations (×). Top: u^+; Bottom: $(u^+_{LES} - u^+)/u^+_{LES}$.

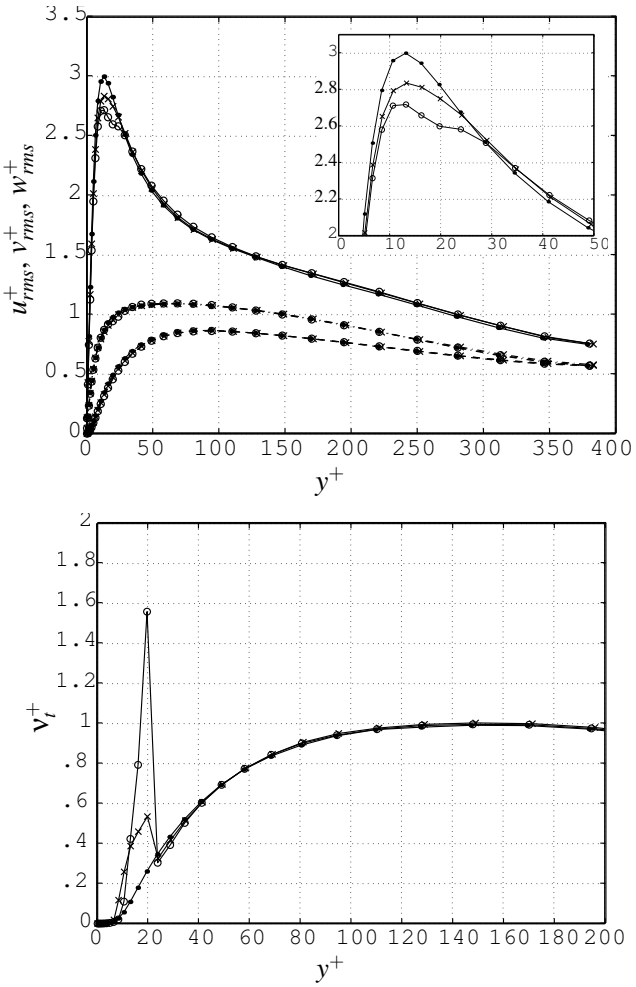

Figure 5. Channel flow at $Re_\tau = 395$. LES (•); LES dynamically coupled with Spalart-Allmaras model equations (○); LES dynamically coupled with k-ω model equations (×). Top: rms velocities; Bottom: ν_t^+.

resolved LES of channel flow at $Re_\tau = 395$. The look-up table for the eddy-viscosity, $\nu_t^+(y^+)$, is obtained from the non-dimensional RANS equation for channel flow $(1 + \nu_t^+)du^+/dy^+ = 1 - y^+/Re_\tau$, where du^+/dy^+ is the gradient of the averaged velocity taken from the LES. This assures that when this eddy-viscosity is used everywhere the averaged velocity profile from LES is recovered. Two additional tables were constructed by storing the eddy-viscosity from the results of channel flow RANS computations using Spalart-Allmaras and k-ω models (decribed in Appendix A). All three RANS eddy-viscosity profiles are shown in Fig. 1. Note that the eddy-viscosities are quite different both in the center of the channel and near the wall (see zoom in Fig. 1).

These tables can be used throughout the channel to compute a RANS solution. The corresponding velocity profiles are shown on the bottom of Fig. 1 with some differences observed in the buffer and the logarithmic layer.

Next, these RANS eddy-viscosity tables are used to compute $\nu_t^{SGS,NW}$ in the near-wall region of the LES simulation. This near-wall region extends up to $y^+ = 20$ (first 12 cells above the wall). Results for all three tables and a traditional LES are presented in Figs. 2-3. The velocity profiles computed with all three tables compare well with the LES. Interestingly, the spread in the velocity profiles for all four computations is smaller than for the three RANS computations presented in Fig. 1. The corrected eddy-viscosity $\nu_t^{SGS,NW}$ dynamically adjusts independent of the near-wall RANS table.

A closer look at the relative error $(u^+_{LES} - u^+)/u^+_{LES}$ reveals that the LES-based table has the smallest error in the logarithmic region. However, the error for all computations is relatively small

Copyright © 2006 by ASME

Downloaded From: https://proceedings.asmedigitalcollection.asme.org on 07/01/2019 Terms of Use: http://www.asme.org/about-asme/terms-of-use

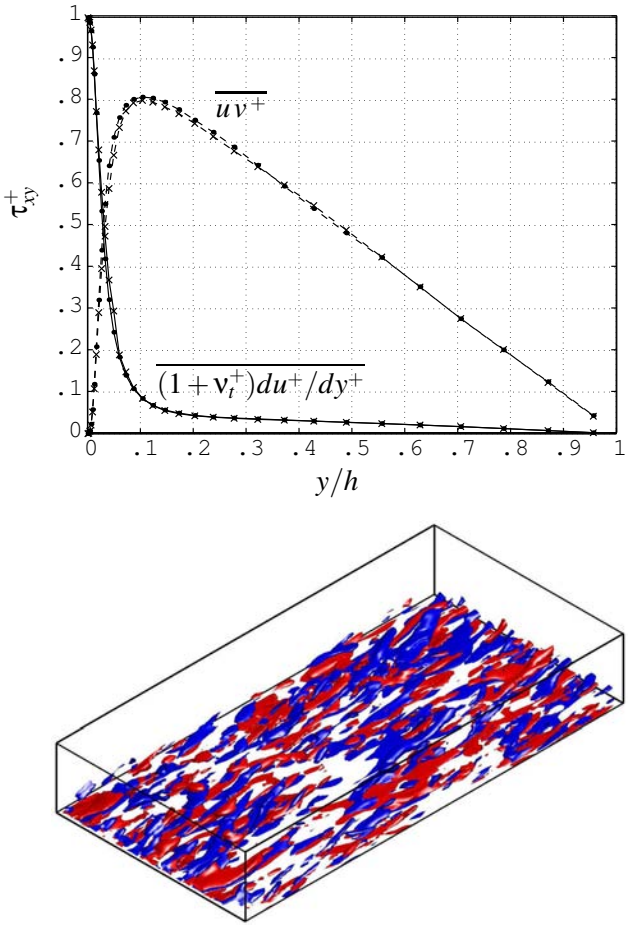

Figure 6. Channel flow at $Re_\tau = 395$. LES (•); LES + $\nu_t^{SGS,NW}$ with dynamic coupling with k-ω model equations (×). Stress balance (left) and isosurfaces of instantaneous streamwise vorticity ω_x (right).

(less than 1% in the logarithmic layer), which suggests that the use of eddy-viscosity coming from RANS turbulence models is appropriate to be used with this approach. Note that the error is largest where the switch from the near-wall treatment to full LES occurs, as shown in the plots for the eddy-viscosity in the same figure. This also affects the peak in the u_{rms} velocity.

Dynamic Coupling With RANS Model Equations

This section describes a dynamic coupling procedure for LES with RANS turbulence model equations. A RANS turbulence model is solved simultaneously with the LES simulation. The LES provides an averaged velocity $\bar{\tilde{u}}$ that is used to compute the convection and production terms in the RANS turbulence model equations. For example, for the k-ω model the equations

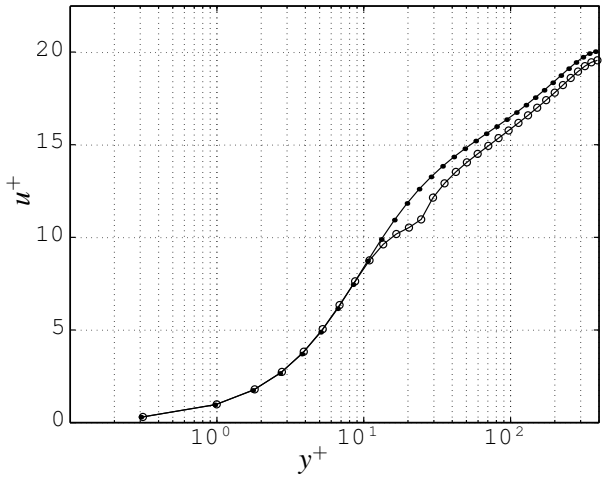

Figure 7. Channel flow at $Re_\tau = 395$. LES (•); LES dynamically coupled with Spalart-Allmaras model without the correction in equation (3) (○). Mean velocity u^+.

are:

$$\frac{\partial k}{\partial t} + \bar{\tilde{u}}_j \frac{\partial k}{\partial x_j} = P_k - C_\mu \omega k + \frac{\partial}{\partial x_j}\left((\nu + \sigma_k \nu_t)\frac{\partial k}{\partial x_j}\right) \qquad (4)$$

$$\frac{\partial \omega}{\partial t} + \bar{\tilde{u}}_j \frac{\partial \omega}{\partial x_j} = \frac{\gamma\omega}{k} P_k - \beta\omega^2 + \frac{\partial}{\partial x_j}\left((\nu + \sigma_\omega \nu_t)\frac{\partial \omega}{\partial x_j}\right) \qquad (5)$$

$$P_k = 2\nu_t S_{ij} S_{ij}, \qquad S_{ij} = \frac{1}{2}\left(\frac{\partial \bar{\tilde{u}}_i}{\partial x_j} + \frac{\partial \bar{\tilde{u}}_j}{\partial x_i}\right) \qquad (6)$$

In the case of channel flow, it is convenient to use plane-averaging to compute $\bar{\tilde{u}}$.

The RANS turbulence model provides ν_t^{rans} which is then corrected with the resolved turbulent stress using equation (3) and used in the near-wall region in the LES.

Results for LES dynamically coupled with Spalart-Allmaras and k-ω turbulence models are compared to LES in Figs. 4 and 5. These results differ only slightly from the results obtained with the precomputed tables presented in Figs. 2-3. However, as can be seen from the relative error for u^+, a stronger variation is observed near the switching point with the dynamic coupling. Interestingly, the dynamic coupling with k-ω produces a smaller jump in the eddy-viscosity at the switching location when compared to results with the precomputed k-ω table. The u_{rms} velocity is also slightly closer to the traditional LES.

Copyright © 2006 by ASME

Downloaded From: https://proceedings.asmedigitalcollection.asme.org on 07/01/2019 Terms of Use: http://www.asme.org/about-asme/terms-of-use

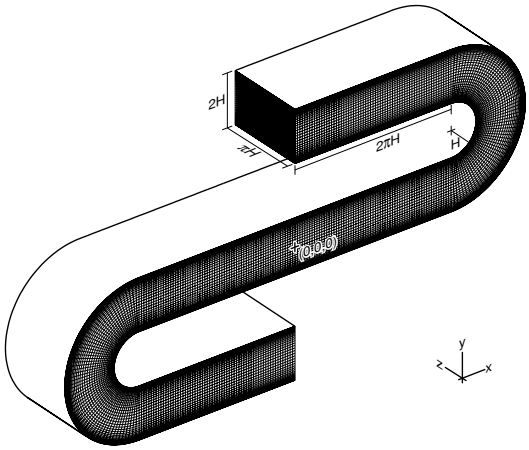

Figure 8. Computational grid for the serpentine passage

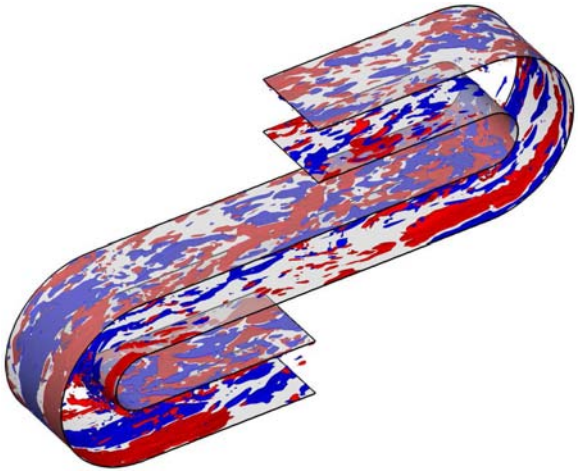

Figure 9. Serpentine passage at $Re_\tau = 180$, LES dynamically coupled with the Spalart-Allmaras model. Isosurfaces of the instantaneous streamwise vorticity $\omega_x = 35$.

The stress balance of resolved stress, $\overline{uv}^+$ and viscous and modeled stress, $(1+\nu_t^+)du^+/dy^+$, presented in Fig. 6, reveals that the resolved stress computed with the dynamic coupling with the k-ω model equations in the near-wall region practically coincides with the results from the LES. The isosurfaces of the instantaneous streamwise vorticity computed using the same approach are also presented in the same figure. This plot illustrates that the near-wall treatment for LES retains coherent turbulent structures.

Note that the dynamic coupling of LES with RANS turbulence model equations was also tested without the correction (3), i.e with RANS eddy-viscosity, ν_t^{rans}, in the near-wall region. In such computations, the abrupt changes of the mean velocity profiles at the switching location (at $y^+ = 20$) were more pronounced, leading to an excess production of turbulence and instabilities. A result for the Spalart-Allmaras model is presented in Fig. 7. This indicates that the correction with the resolved stress in equation (3) is a key element in the coupling procedure.

SERPENTINE PASSAGE

The channel flow, analyzed in the previous section, represents a proof of concept for the proposed dynamic coupling of LES with RANS turbulence models in the near-wall region. A more challenging application is the serpentine passage, computed using DNS in [4]. Although periodic in the streamwise and spanwise directions, this problem offers increased complexity over channel flow due to the curved walls, changing pressure gradients and separation. The geometry is typical of internal cooling passages in gas turbine blades. Accurate flow predictions in these passages are necessary to improve their design.

Although this geometry appears relatively simple, it is well-known that RANS turbulence models have difficulties accurately predicting the critical flow features. LES has been shown to significantly improve the results for these flows, but the computational cost is prohibitive for higher Reynolds numbers. The aim of coupling LES with RANS turbulence models in the near-wall region is to allow the use of grids coarsened in wall-parallel directions, while preserving the accuracy of LES.

The geometry and the computational grid are presented in Fig. 8. The height of the channel is $2H$, the length of the straight part of the passage upstream of the bend is $2\pi H$ and the inner radius of the bend is H. The width in the spanwise direction was set to πH. The Reynolds number based on the bulk velocity, U_b, is $Re_b = U_b H/\nu = 2800$ which corresponds to $Re_\tau = 180$. The computational grid consists of 384x48x48 cells in the streamwise, wall-normal and spanwise directions, respectively. A two-dimensional version of the same grid is used for RANS computations with 384x48 cells. The average y^+ of the first cell centers is about 0.5 with a maximum value of 1.0.

RANS turbulence models poorly predict this flow, as illustrated by the comparison of skin friction and pressure coefficients computed using the Spalart-Allmaras and k-ω models with the DNS in Fig. 10. In contrast, the results computed with LES agree well with the DNS, as shown in Fig. 11.

An important feature of this flow is the separation encoun-

Table 1. Mean separation characteristics.

	SA	k-ω	LES	DNS [4]
separation angle	105.66^o	115.93^o	133.68^o	140.01^o
x reattachment	2.00	3.38	4.81	4.86
bubble height	10.36%	7.74%	4.37%	5.02%

Copyright © 2006 by ASME

Downloaded From: https://proceedings.asmedigitalcollection.asme.org on 07/01/2019 Terms of Use: http://www.asme.org/about-asme/terms-of-use

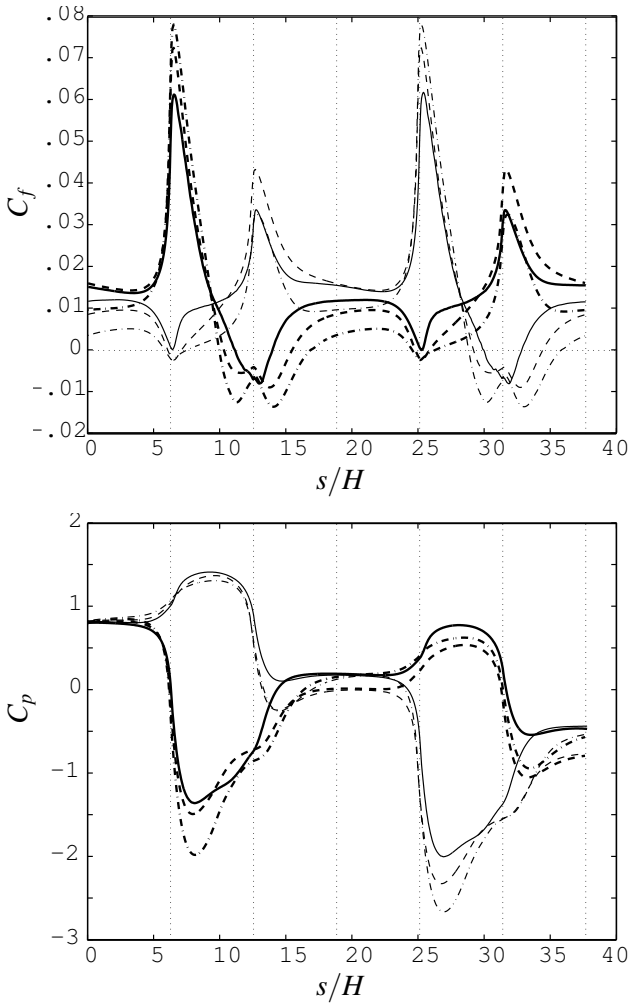

Figure 10. Serpentine passage at $Re_\tau = 180$. Skin friction (top) and pressure (bottom) coefficient. RANS with Spalart-Allmaras model (dash-dotted), k-ω model (dashed) and DNS [4] (solid) along both inner (thick) and outer walls (thin).

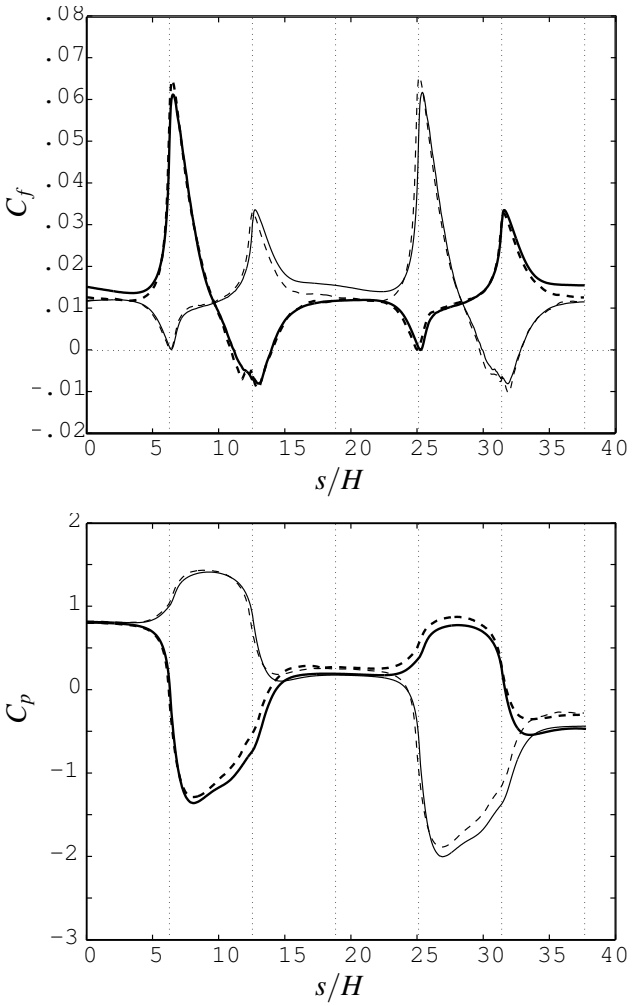

Figure 11. Serpentine passage at $Re_\tau = 180$. Skin friction (top) and pressure coefficient (bottom) for LES (dashed) and DNS [4] (solid) along both inner (thick) and outer walls (thin).

tered along the inner walls downstream of the bends. The mean separation characteristics are presented in Table 1. The corresponding streamlines are shown in Fig. 12. Clearly, RANS models predict the separation too early and are overpredicting the size of the recirculating region.

The discrepancies in the skin friction distribution between RANS and LES can be explained in part by predictions of turbulent kinetic energy. Contours of turbulent kinetic energy computed using the k-ω model and LES are presented in Fig. 13.

Next, we consider the near-wall treatment for LES that uses the dynamic coupling with RANS turbulence models (Spalart-Allmaras and k-ω). For the serpentine passage, the equation (3) can still be applied as long as the quantities $\overline{\hat{u}'\hat{v}'}$ and $d\bar{\hat{u}}/dy$ are defined in a local coordinate system aligned with the wall. In practice, $\overline{\hat{S}}_{ij}$ and $\overline{\hat{u}'_i\hat{u}'_j}$ are computed in the general coordinate system and are then expressed in the local coordinate system. In these computations, the RANS eddy-viscosity is obtained from a simultaneous solution of RANS turbulence model equations that use $\bar{\hat{u}}$ from the LES. The averaging for all quantities is performed in the spanwise direction combined with time-averaging.

The computations using dynamic coupling with the Spalart-Allmaras model are performed on the same wall-resolved grid used for the LES. The near-wall region extends up to $y/H = 0.2$, (y being the distance to the wall). The results are presented in Figs. 14- 15. The flow separates at 129^o, reattaches at $x = 4.80$ and the bubble height is 5.44%; i.e. the separation is slightly larger than when computed with the LES. The near-wall coupling has only minimal effects on the LES solution. Interestingly, the effect of the LES on the RANS turbulence model equations,

Copyright © 2006 by ASME

Downloaded From: https://proceedings.asmedigitalcollection.asme.org on 07/01/2019 Terms of Use: http://www.asme.org/about-asme/terms-of-use

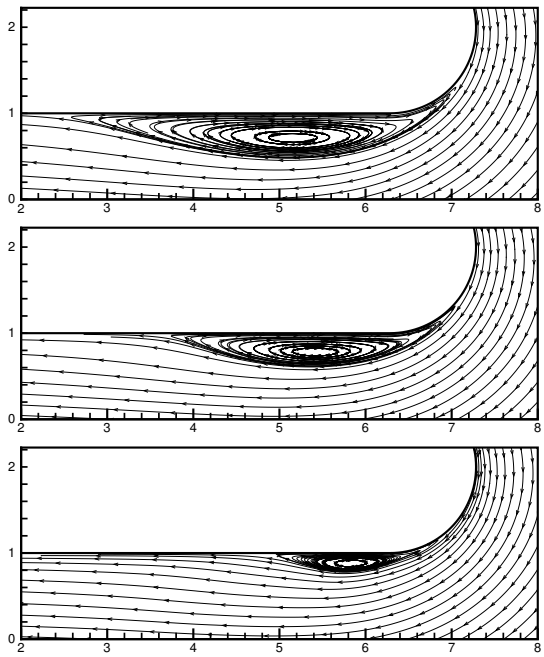

Figure 12. Serpentine passage at $Re_\tau = 180$. Top: Spalart-Allmaras; Middle: k-ω; Bottom: LES. Mean flow streamlines.

via $\tilde{\tilde{u}}$, is much larger. It significantly reduces the RANS eddy-viscosity as compared to the stand-alone RANS solution.

CONCLUSIONS

The RANS/LES coupling formulation proposed in [1–3] has been adapted for use with various RANS turbulence models. That formulation consists of imposing a RANS eddy-viscosity dynamically corrected with the resolved turbulent stress near the wall.

The RANS eddy-viscosity can be obtained from precomputed tables, as well as by solving the RANS turbulence model equations simultaneously. Results obtained for channel flow at $Re_\tau = 395$ using the dynamic coupling with the Spalart-Allmaras and k-ω model equations are in good agreement with the traditional LES.

The proposed dynamic coupling is then applied to a serpentine passage and compared with DNS computations [4] at $Re_\tau = 180$. Despite the presence of the separation and pressure gradients, the results agree well with the LES. To investigate the computational advantages of this approach, the flow in the serpentine passage will be computed for higher Reynolds numbers and compared to available experimental data.

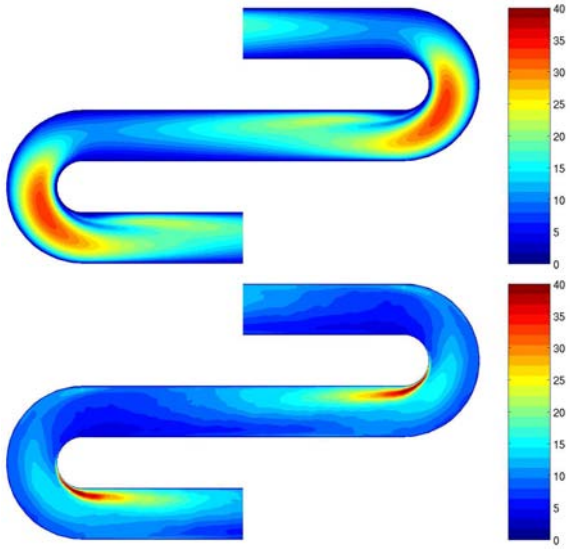

Figure 13. Serpentine passage at $Re_\tau = 180$. Top: RANS with k-ω model; Bottom: LES. Turbulent kinetic energy.

ACKNOWLEDGMENT

This research was sponsored by Belgian American Educational Foundation (BAEF), GE Aircraft Engines through the USA program, the AFOSR Grant # F49620-03-1-0132 and by the DOE through the ASC program at CITS.

Computer time was provided by the Center for Research in Aeronautics (CENAERO) financially supported from the Walloon region (DGTRE) and the European Union (FEDER and DSE). The first author was visiting the Center for Turbulence Research at Stanford University while this work was performed.

REFERENCES

[1] Kalitzin, G., Templeton, J., and Medic, G., 2005. *A near-wall eddy-viscosity formulation for LES*. Proceedings of Symposium on Complex Effects in Large Eddy Simulations, Springer Verlag, Heidelberg.

[2] Medic, G., Templeton, J., and Kalitzin, G., 2005. "A formulation for near-wall RANS/LES coupling". *J. Comp. Phys.*, p. (In press).

[3] Templeton, J., Medic, G., and Kalitzin, G., 2005. "An eddy-viscosity based near-wall treatment for coarse grid LES". *Phys. Fluids,* **17**(105101).

[4] Laskowski, G., 2005. "Inverse design of a turbine cascade passage and DNS of a stationary and rotating serpentine passage". PhD thesis, Stanford University.

[5] Baggett, J., Jimenez, J., and Kravchenko, A., 1997. "Resolution requirements in large-eddy simulation of shear flows". *CTR Annual Research Briefs*, pp. 51–66.

[6] Balaras, E., Benocci, C., and Piomelli, U., 1996. "Two-

Copyright © 2006 by ASME

Downloaded From: https://proceedings.asmedigitalcollection.asme.org on 07/01/2019 Terms of Use: http://www.asme.org/about-asme/terms-of-use

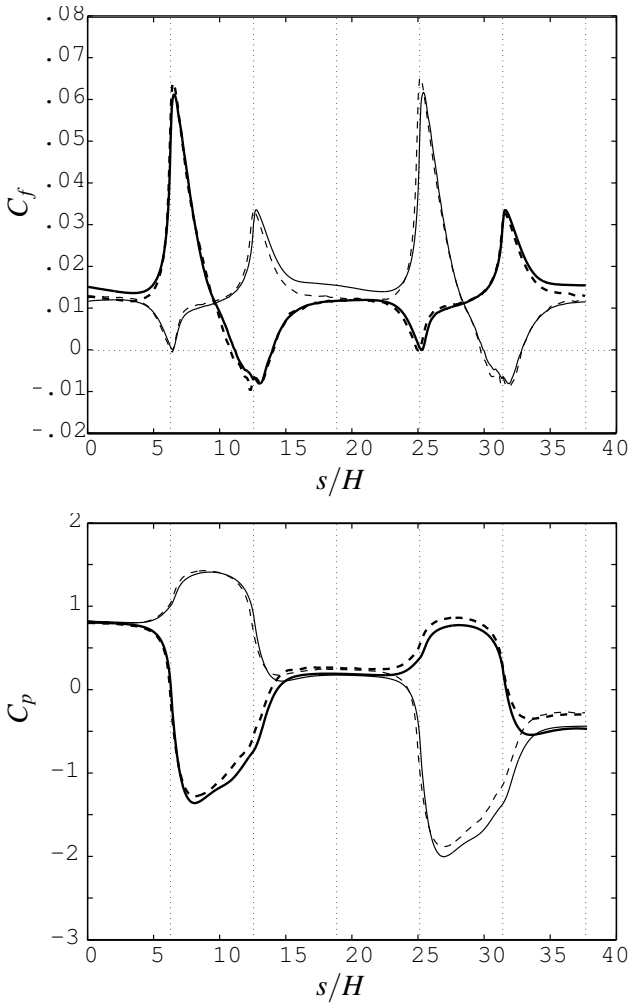

Figure 14. Serpentine passage at $Re_\tau = 180$. Skin friction (top) and pressure coefficient (bottom) for LES dynamically coupled with the Spalart-Allmaras model (dashed) and DNS [4] (solid) along both inner (thick) and outer walls (thin).

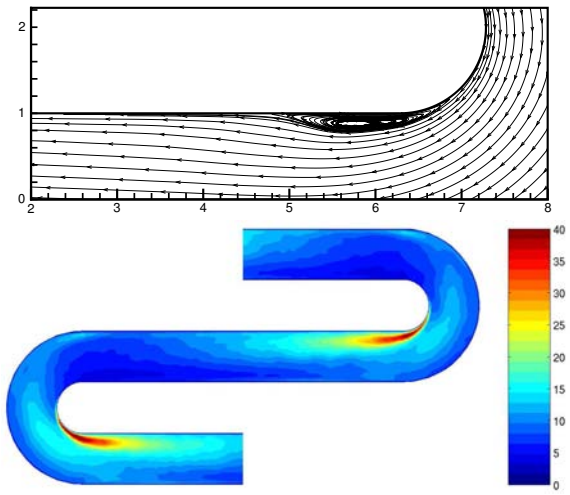

Figure 15. Serpentine passage at $Re_\tau = 180$. LES dynamically coupled with the Spalart-Allmaras model. Top: Mean flow streamlines; Bottom: Turbulent kinetic energy.

layer approximate boundary conditions for large-eddy simulations". *AIAA Jounal,* **34**, pp. 1111–1119.

[7] Cabot, W., and Moin, P., 2000. "Approximate wall boundary conditions in the large-eddy simulation of high Reynolds number flow". *Flow, Turbulence and Combustion,* **63**, pp. 269–291.

[8] Wang, M., and Moin, P., 2002. "Dynamic wall modeling for large-eddy simulation of complex turbulent flows". *Phys. Fluids,* **14**(7), pp. 2043–2051.

[9] Spalart, P., Jou, W.-H., Strelets, M., and Allmaras, S., 1997. *Comments on the feasibility of LES for wings, and on a hybrid RANS/LES approach*. First AFOSR International Conference on DNS/LES, Ruston, LA, pp. 4–8.

[10] Nikitin, N., Nicoud, F., Wasistho, B., Squires, K., and Spalart, P., 2000. "An approach to wall modelling in large-eddy simulations". *Phys. Fluids. Letters,* **12**(7), p. 1629.

[11] Wilcox, D., 1993. *Turbulence modeling for CFD*. DCW Industries, La Canada, California.

[12] Spalart, P., and Allmaras, S., 1994. "A one-equation turbulence model for aerodynamic flows". *La Recherche Aerospatiale,* **1**, pp. 1–23.

[13] Wu, X., and Durbin, P., 2001. "Evidence of longitudinal vortices evolved from distorted wakes in a turbine passage". *J. Fluid Mech.,* **446**, pp. 199–228.

[14] Rosenfeld, M., Kwak, D., and Vinokur, M., 1991. "A fractional-step solution method for the unsteady incompressible Navier-Stokes equations in generalized coordinate systems". *J. Comp. Phys.,* **94**(1), pp. 102–137.

[15] Nicoud, F., and Ducros, F., 1999. "Subgrid-scale stress modelling based on the square of the velocity gradient tensor". *Flow, Turbulence and Combustion,* **62**(3), pp. 183–200.

[16] Kalitzin, G., Medic, G., Iaccarino, G., and Durbin, P., 2005. "Near-wall behavior of RANS turbulence models and implications for wall functions". *J. Comp. Phys.,* **204**(1), pp. 265–291.

Copyright © 2006 by ASME

Downloaded From: https://proceedings.asmedigitalcollection.asme.org on 07/01/2019 Terms of Use: http://www.asme.org/about-asme/terms-of-use

Appendix A: RANS Turbulence Models

Spalart-Allmaras turbulence model

The Spalart-Allmaras model [12] consists of one transport equation

$$\partial_t \tilde{\nu} + u \cdot \nabla \tilde{\nu} = Q(\tilde{\nu}) + \frac{c_{b2}}{c_{b3}} \nabla \tilde{\nu} \cdot \nabla \tilde{\nu} + \frac{1}{c_{b3}} \nabla \cdot [(\nu + \tilde{\nu}) \nabla \tilde{\nu}] \quad (7)$$

where the source term $Q(\tilde{\nu})$ is

$$Q(\tilde{\nu}) = c_{b1}(1 - f_{t2}) \tilde{S} \tilde{\nu} + (\frac{c_{b1}}{\kappa^2} f_{t2} - c_{w1} f_w) \left(\frac{\tilde{\nu}}{d} \right)^2 \quad (8)$$

The eddy-viscosity is

$$\nu_t = \tilde{\nu} f_{v1} \quad (9)$$

The model damping functions, auxiliary relations and the trip term are defined as:

$$f_{v1} = \frac{\chi^3}{\chi^3 + {c_{v1}}^3}, \quad f_{v2} = 1 - \frac{\chi}{1 + \chi f_{v1}}, \quad \chi = \frac{\tilde{\nu}}{\nu} \quad (10)$$

$$f_w = g \left[\frac{1 + {c_{w3}}^6}{g^6 + {c_{w3}}^6} \right]^{\frac{1}{6}}, \quad g = r + c_{w2}(r^6 - r), \quad r = \frac{\tilde{\nu}}{\tilde{S} \kappa^2 d^2} \quad (11)$$

$$\tilde{S} = S + \frac{\tilde{\nu}}{\kappa^2 d^2} f_{v2}, \quad S = \sqrt{2 S_{ij} S_{ij}}, \quad f_{t2} = c_{t3} \exp(-c_{t4} \chi^2) \quad (12)$$

The variable d is the distance to the nearest wall, κ the von Kármán constant and the strain rate tensor is $S_{ij} = \frac{1}{2}(\partial_j u_i + \partial_i u_j)$. Finally, the model closure coefficients are

$$c_{b1} = 0.1355, \quad c_{b2} = 0.622, \quad c_{b3} = 2/3, \quad c_{v1} = 7.1 \quad (13)$$

$$c_{w1} = \frac{c_{b1}}{\kappa^2} + \frac{1 + c_{b2}}{c_{b3}}, \quad c_{w2} = 0.3, \quad c_{w3} = 2, \quad c_{t3} = 1.2, \quad c_{t4} = 0.5 \quad (14)$$

The wall boundary condition is:

$$\tilde{\nu} = 0 \quad (15)$$

k-ω model

In the Wilcox's original k-ω model [11], the eddy-viscosity is defined as:

$$\nu_t = k/\omega \quad (16)$$

The equation for turbulent kinetic energy is

$$\partial_t k + u \cdot \nabla k = P_k - C_\mu \omega k + \nabla \cdot [(\nu + \sigma_k \nu_t) \nabla k] \quad (17)$$

where

$$P_k = \nu_t S^2, \qquad S = \sqrt{2 S_{ij} S_{ij}} \quad (18)$$

The equation for the specific dissipation rate ω is:

$$\partial_t \omega + u \cdot \nabla \omega = \frac{\gamma \omega}{k} P_k - \beta \omega^2 + \nabla \cdot [(\nu + \sigma_\omega \nu_t) \nabla \omega]. \quad (19)$$

The original model constants are

$$\sigma_k = \sigma_\omega = 0.5; \ \gamma = 5/9; \ \beta = 0.075; \ C_\mu = 0.09.$$

The wall boundary condition for k is:

$$k = 0. \quad (20)$$

At the wall, the specific dissipation rate ω asymptotically tends to infinity as $\sim 1/y^2$. The boundary condition used here is

$$\omega = \frac{60\nu}{\beta d_1^2} \quad (21)$$

where d_1 is the distance from the wall to the cell center of the first cell above the wall.

Appendix B: Wall Adapting Local Eddy-Viscosity Model (WALE)

The WALE subgrid-scale model developed in [15] was implemented. It is an eddy-viscosity model based on the square of the velocity gradient tensor and accounts for the effects of both the strain and the rotation rate to obtain the local eddy-viscosity. Its greatest advantage is that it recovers the proper y^3 near-wall scaling for the eddy-viscosity without requiring a dynamic procedure.

Copyright © 2006 by ASME

Downloaded From: https://proceedings.asmedigitalcollection.asme.org on 07/01/2019 Terms of Use: http://www.asme.org/about-asme/terms-of-use

The WALE model eddy-viscosity is given by:

$$\nu_t = (C_w \Delta)^2 \frac{\left(\mathcal{S}^d_{ij}\mathcal{S}^d_{ij}\right)^{3/2}}{\left(\overline{S}_{ij}\overline{S}_{ij}\right)^{5/2} + \left(\mathcal{S}^d_{ij}\mathcal{S}^d_{ij}\right)^{5/4}} \tag{22}$$

where $\overline{S}_{ij}$ is the strain rate tensor for the resolved field. $\mathcal{S}^d_{ij}$ is defined as follows:

$$\mathcal{S}^d_{ij} = \frac{1}{2}\left(\overline{g}^2_{ij} - \overline{g}^2_{ji}\right) - \frac{1}{3}\delta_{ij}\overline{g}^2_{kk}, \tag{23}$$

with $\overline{g}^2_{ij} = \frac{\partial \overline{u}_i}{\partial x_k}\frac{\partial \overline{u}_k}{\partial x_j}$ and δ_{ij} the Kronecker symbol. The model constant C_w is here set to 0.5; this value is given in [15] and was calibrated numerically for isotropic decaying turbulence. In these computations the subgrid characteristic length scale Δ is set to the cubic root of the local cell volume.

Copyright © 2006 by ASME

Downloaded From: https://proceedings.asmedigitalcollection.asme.org on 07/01/2019 Terms of Use: http://www.asme.org/about-asme/terms-of-use